Oxidative dehydrogenation of ethane and propane over magnesium–cobalt phosphates $Co_xMg_{3-x}(PO_4)_2$

Abdellah Aaddane, Mohamed Kacimi and Mahfoud Ziyad *

Faculté des Sciences, Département de Chimie, Laboratoire de Physico-Chimie des Matériaux et Catalyse, Avenue Ibn Batouta, BP 1014, Rabat, Morocco
E-mail: ziyad@fsr.ac.ma

Received 11 August 2000; accepted 29 January 2001

The magnesium–cobalt phosphates $Co_xMg_{3-x}(PO_4)_2$ belonging to the olivine-type structure were synthesized by coprecipitation and then investigated in the oxidative dehydrogenation (ODH) of ethane and propane. The best yields, with the exception of $Co_{0.5}Mg_{2.5}(PO_4)_2$, were achieved with the compositions ranging between $1 \leqslant x \leqslant 2.5$. Magnesium phosphate $Mg_3(PO_4)_2$ displayed no activity and pure cobalt phosphate $Co_3(PO_4)_2$ was found to be the less active component of the solid solution. Comparison of the catalysts performances showed that they all have similar activity in ethane and propane ODH, albeit, they are more selective in propylene than in ethylene production. The $Co_xMg_{3-x}(PO_4)_2$ solid solution was also studied, for characterization purposes, in butan-2-ol conversion. The samples presented acid–base properties due essentially to the (PO–H) groups but they do not bear conventional redox centers. All the catalysts were active at low temperatures in the alcohol dehydration. The dehydrogenation activity versus the phosphates composition displayed two maxima around $x = 1$ and 2, respectively. Similar striking behavior was also observed in ethane and propane ODH. UV-visible investigations of $Co_xMg_{3-x}(PO_4)_2$ showed, in agreement with the XRD data, that the Co^{2+} ions are distributed in the phosphate framework between six- and five-coordinated sites. The cobalt atoms in the five-coordinated sites Co(5) and their Co(5)–Co(5) interatomic distances were assumed to play the main role in the C–H bond activation and the appearance of maxima in the activity. Magnesium cations presumably intervene in acid–base properties of the samples and O_2 activation. Characterization of the samples showed that they do not undergo any noticeable transformation after the catalytic tests.

KEY WORDS: cobalt–magnesium phosphates; ethane; propane; oxidative dehydrogenation

1. Introduction

Transition metal phosphates have been widely investigated in heterogeneous catalysis, particularly in reactions requiring acid sites [1–3]. Among this large family of materials aluminum phosphate, $AlPO_4$, is probably the most studied [4,5]. Depending on its composition it might have acid (Al/P < 1), neutral (Al/P = 1) or basic (Al/P > 1) properties. Similar results have been achieved with other phosphates such as BPO_4 or α-ZrP [6,7]. The acid properties of a surface can also be improved by loading it with different amounts of sulfates, boron, P_2O_5, or organic compounds for enantioselective hydrogenations [8–11]. The resulting solids usually exhibit enhanced catalytic performances. However, despite these technical improvements of the catalysts, the description of the active sites and the understanding of the catalytic processes requires the use of solids with well defined structures in order to minimize irrelevant interpretations.

Selective oxidation and oxidative dehydrogenation of light alkanes represent an important economic issue and a scientific challenge in heterogeneous catalysis. Several studies have been recently carried out over many phosphorus based catalysts [12–14]. However, except for *n*-butane conversion to maleic anhydride on vanadium phosphorus oxides (VPO), only few solids exhibited reasonable selectivity [15]. Suitable catalytic conditions for C–H bond activation in light alkanes are not as yet entirely known. The breaking of the C–H bond is probably not the main difficulty. It is rather the stability of the reaction products at high temperatures that limits the yields. Moreover, light alkanes are known to easily exchange their hydrogen atoms for deuterium on appropriate catalysts at relatively low temperatures [16]. The literature also reported that transition metals adsorb light alkanes (e.g., CH_4) producing carbonaceous deposits on the catalyst surface and alkyl species by the removal of hydrogen from the hydrocarbon [17,18]. A subsequent hydrogenation of these deposits leads in some cases to higher alkanes. Therefore, one may presume that the light alkanes activation does not only depend on the strength of the C–H bond but also on the composition of the catalyst and its structural features. A variety of phosphates have been examined as catalysts for the light alkanes activation and promising results were recently reported in the literature [13,19].

The present study is devoted to the investigation of the catalytic properties of cobalt–magnesium phosphates $Co_xMg_{3-x}(PO_4)_2$ ($0 \leqslant x \leqslant 3$) prepared by coprecipitation in the oxidative dehydrogenation of ethane and propane. The acid properties and the redox behavior of this solid solution were also studied in butan-2-ol conversion. Attempts to correlate the catalytic activity and selectivity in both reactions to the structural properties of the samples were undertaken and special attention was given to the catalysts characterization before and after the catalytic tests.

* To whom correspondence should be addressed.

1011-372X/01/0400-0047$19.50/0

Table 1
Surface areas of the catalysts $Co_xMg_{3-x}(PO_4)_2$ calcined at 550 and 700 °C.

	x						
	0	0.5	1	1.5	2	2.5	3
Area at 550 °C ($m^2\,g^{-1}$)	57.8	11.8	21.6	13.8	9.8	12.7	9.3
Area at 700 °C ($m^2\,g^{-1}$)	8.3	6.5	4.6	7.3	3.7	3.8	2

2. Experimental

Several compositions of the solid solution $Co_xMg_{3-x}(PO_4)_2$ (with $0 \leqslant x \leqslant 3$) were prepared by coprecipitation in aqueous media by adding to a solution of $(NH_4)_2HPO_4$ stoichiometric quantities of $Mg(NO_3)_2{\cdot}6H_2O$ and $Co(NO_3)_2{\cdot}6H_2O$ separately dissolved in water. The precipitate was kept under stirring for 1 h and then dried until the water was completely eliminated. For each composition ($x = 0, 0.5, 1, 1.5, 2, 2.5$ and 3), the resulting material was heated overnight at 300 °C, then submitted to repeated cycles of grinding and sintering at 550 and 700 °C.

The specific surface areas of the samples calcined at 550 and 700 °C were measured using nitrogen adsorption at −196 °C. The results are reported in table 1.

X-ray powder diffraction patterns were recorded on a Philips PW 1710 diffractometer using Cu Kα (λ = 0.1542 nm) radiation.

Diffuse reflectance spectra were taken with a Perkin–Elmer (Lambda 9) spectrometer equipped with an integrating sphere and $BaSO_4$ as the reference. The measurements were performed in a cell permitting *in situ* treatments of the samples at the desired temperature.

Butan-2-ol conversion was performed at 220 °C in a microreactor operated at atmospheric pressure. The alcohol was introduced in the reactor diluted in N_2/O_2 (air) at a partial pressure equal to 8.4×10^2 Pa. The total flow rate was equal to 60 cm^{-1} min. Prior to the reaction, 50 mg of the catalyst were evacuated under a pure nitrogen flow for 2 h at 300 °C.

Oxidative dehydrogenation of hydrocarbons was carried out at atmospheric pressure, in a quartz U-shaped reactor. The catalyst, with grains ranging in size from 125 to 180 μm, was placed in the reactor between two quartz-wool plugs. The composition of the feed was 6 vol% of the alkane and 3 vol% of O_2 diluted in nitrogen. The reaction mixture was introduced in the reactor at room temperature with a total flow rate equal to 60 $cm^3\,min^{-1}$. Immediately after, the catalyst temperature was linearly increased (5 °C min^{-1}) until 500 or 550 °C. The products were analyzed on Porapak Q columns using two on line gas chromatographs.

The absence of external and internal mass transport limitations was checked varying (i) the gas flow rate versus the catalyst mass at constant contact time, and (ii) the conversion versus the catalyst grain size. The homogeneous reaction does not start in the selected experimental conditions before 600 °C.

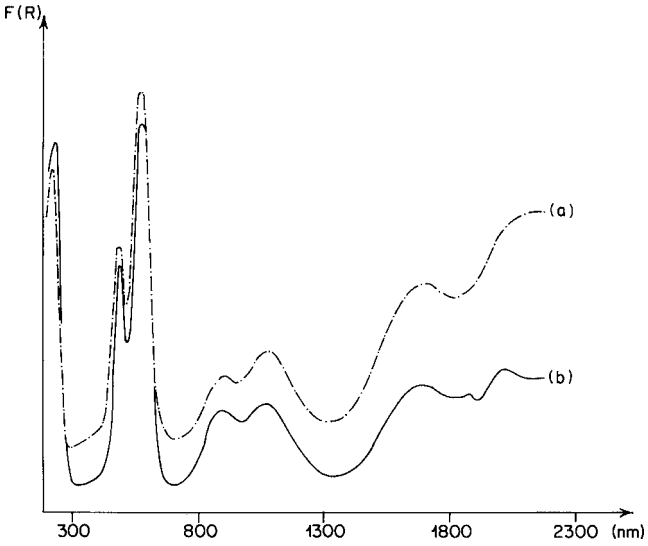

Figure 1. UV-visible spectra of $Co_xMg_{3-x}(PO_4)_2$ ($0 \leqslant x \leqslant 3$), samples calcined at (a) 550 and (b) 700 °C.

3. Results and discussion

3.1. Catalysts characterization

X-ray diffraction patterns of cobalt–magnesium $Co_xMg_{3-x}(PO_4)_2$ ($0 \leqslant x \leqslant 3$) phosphates calcined at 700 °C are similar to those reported in the literature [20]. Both phosphates, $Co_3(PO_4)_2$ and $Mg_3(PO_4)_2$, are isostructural and completely soluble in each other over the entire composition range. Their structure belongs to the olivine-type and is mainly built up of $(Co,Mg)O_5$, $(Co,Mg)O_6$ and (PO_4) polyhedra shearing corners [21]. The samples calcined at 550 °C exhibit a weak level of crystallization. Their purity was checked by IR spectroscopy and chemical analysis. IR spectra confirmed the absence of pyrophosphate $(P_2O_7)^{4-}$ groups which are characterized by a P–O–P vibration around 725 cm^{-1}.

UV-visible spectra of the samples calcined at 550 °C displayed several bands in the near infrared at 2100, 1700, 1100 and 900 nm and in the visible region at 450–600 nm (figure 1(a)). The assignment of these bands was based on the structural properties of $Co_xMg_{3-x}(PO_4)_2$. Those appearing at 2100, 1080 and 580 nm were attributed to the Co^{2+} ions in octahedral coordination. Those located at 1700, 900 and 490 nm by comparison with the spectrum of [Co(trenMe)Cl]Cl were assigned to Co^{2+} ions in a trigonal environment [22]. The single band centered on 235 nm was attributed to $O^{2-} \rightarrow Co^{2+}$ and $O^{2-} \rightarrow Mg^{2+}$ charge transfers. All the spectra of the solid solution showed identical profiles, presumably because the energies of the transitions do not change with the cobalt concentration in the samples. When the phosphates are calcined at 700 °C, the two bands centered at 900 and 1100 nm are better resolved (figure 1(b)). These bands, as reported in the literature, result from Co^{2+} ions located in a trigonal bipyramidal and in an octahedral environment, respectively. Their relative intensities showed a slight tendency of Co^{2+} ions to prefer-

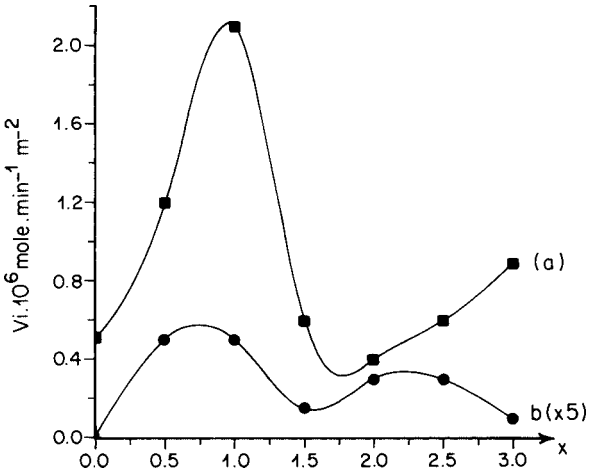

Figure 2. Rates of butan-2-ol dehydration (a) and dehydrogenation (b) versus $Co_xMg_{3-x}(PO_4)_2$ composition at 220 °C. The samples were calcined at 550 °C.

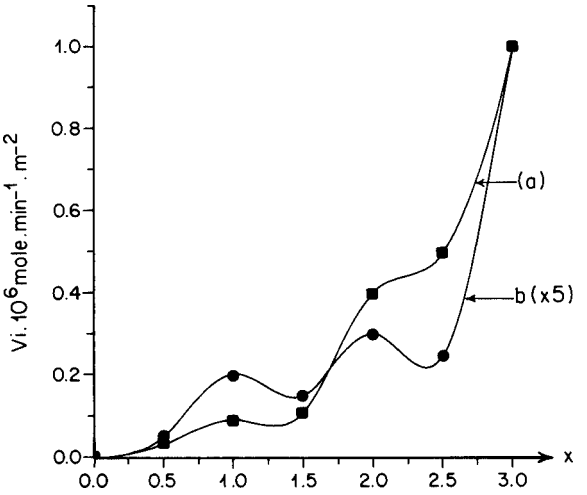

Figure 3. Rates of butan-2-ol dehydration (a) and dehydrogenation (b) versus $Co_xMg_{3-x}(PO_4)_2$ composition at 220 °C. The samples were calcined at 700 °C.

ably occupy the five coordinated sites rather than the six-coordinated sites. This distribution does not seem to be affected by an increase of Co^{2+} ion concentration in the phosphate. Neither did the samples, before or after the catalysis runs, exhibit any presence of Co^{3+} ions which are characterized in octahedral environments by d–d transition bands around 400 and 700 nm [23].

3.2. Butan-2-ol conversion

It was pointed out that the mechanism of the oxidative dehydrogenation of light alkanes involves redox and acid–base sites [24]. Investigation of these sites on $Co_xMg_{3-x}(PO_4)_2$ was carried out using butan-2-ol conversion in presence of O_2. The reaction produces butenes by dehydration on acid centers and methyl ethyl ketone on basic or redox sites. Figure 2 displays the achieved activity versus the composition at 220 °C on samples calcined at 550 °C. It shows (figure 2(a)) that the rate of butan-2-ol conversion to butenes goes through a maximum located at $x = 1$, then it decreases and increases again until $x = 3$. $Mg_3(PO_4)_2$ is only active in the dehydration reaction while $Co_3(PO_4)_2$ is active in the dehydration as well as in the dehydrogenation. The dehydrogenation activity shows two distinct maxima for the compositions $x = 0.75$ and 2.25 (figure 2(b)). When the catalysts are calcined at 700 °C, the dehydration and the dehydrogenation activities also displayed two maxima at $x = 1$ and 2 (and a much higher activity at $x = 3$) (figure 3). The shift of the maxima positions while increasing the calcination temperature is probably related to the completion of the samples crystallization and the surface atoms organization. At this calcination temperature pure magnesium phosphate is inactive and adsorption of acetic acid or pyridine on it shows that it only possesses weak acid–base sites that disappear completely after an evacuation above 350 °C [25]. However, enrichment of $Mg_3(PO_4)_2$ with Co leads to catalysts active in the dehydration and the dehydrogenation. Therefore, it might be assumed that all the $Mg_{3-x}Co_x(PO_4)_2$ ($0 < x < 3$) phosphates exhibit, in the temperature range where butan-2-ol was converted, a Brønsted acidity that participates in the dehydration reaction. Beside these acid centers, the system also bears basic sites probably constituted by the negative charges located on the oxygen atoms of the $(PO_4)^{3-}$ groups and on the Co^{2+} cations [26]. It was shown in the literature by EPR technique, in the similar case of CoO–MgO solid solution, that superoxo radicals are formed on Co^{2+} and spill over Mg^{2+} cations [27]. It is probably those O_2^-, O^- and O^{2-} species that act as the redox sites in the dehydrogenation to produce methyl ethyl ketone. The amount of these charged oxygen species varies with the phosphate content in cobalt and magnesium and consequently modifies the catalytic properties of the catalysts. The optimal concentrations of these active species are probably reached when the catalysts compositions are around $x = 1$ and 2.

The existence of the maxima of activity reveals, on the other hand, a sensitivity of butan-2-ol conversion to the catalysts composition. As a matter of fact, the $Co_xMg_{3-x}(PO_4)_2$ solid solution undergoes modifications of the length of the Co(5)–Co(5) interatomic distance when the solid solution is enriched with cobalt [28]. If it is assumed that the alcohol adsorbs on two adjacent cobalt bearing oxygen atoms the activity variations might be then related to the presence on the catalysts surface of correctly spaced atoms that can accommodate butan-2-ol adsorption and conversion [29]. The distance between the C_α carbon and the oxygen of the OH function in butan-2-ol is approximately equal to 3.18 Å. Therefore, the best catalytic results should be obtained when using phosphates that exhibit Co(5)–Co(5) interatomic distances lying around 3.18 Å. The experimental results indicate that the compositions $x = 1, 2$ and 3 should have adequate Co(5)–Co(5) distances (figures 2 and 3). The crystallographic positions of cobalt ions in the solid solution $Co_xMg_{3-x}(PO_4)_2$ ($0 \leqslant x \leqslant 3$) confirmed that $x = 2$ and 3 have Co(5)–Co(5) distances equal to 3.00 and 3.062 Å, respectively [21]. For $x = 1$, the structure has not been yet resolved and the Co(5)–Co(5) distance is not available.

However, we can reasonably admit that it is superior to 3 Å. All the other compositions display Co(5)–Co(5) distances inferior to 3 Å and consequently low performances. This interpretation of the results assumes that the Co(5)–Co(5) distances on the catalyst surface are identical to that existing in the bulk.

In view of the complexity and the intriguing character of the results presented here, all the experiments have been reproduced several times on each composition in order to minimize the errors and authenticate the observed phenomena.

3.3. Oxidative dehydrogenation of C_2H_6

Under the experimental conditions used the reaction starts around 450 °C and produces only ethylene and CO_x. The conversions and the selectivities achieved at the steady state for various compositions of $Mg_{3-x}Co_x(PO_4)_2$ calcined at 550 °C are displayed in figure 4. The reaction temperatures investigated are 500 and 550 °C. Magnesium phosphate is inactive. However, as its content of Co^{2+} ions is increased, the ethylene conversion rapidly increases to reach 34% for $x = 1$. It stays around that level with a C_2H_4 selectivity approaching 45% until the composition $x = 2.5$, where the conversion becomes 36.6% and the selectivity 44%. Pure $Co_3(PO_4)_2$ unexpectedly exhibited a much lower activity (13%) and a selectivity of 55%. At the reaction temperature equal to 500 °C the activity is lower than at 550 °C but it clearly exhibits two maxima located at $x = 1$ and 2.5.

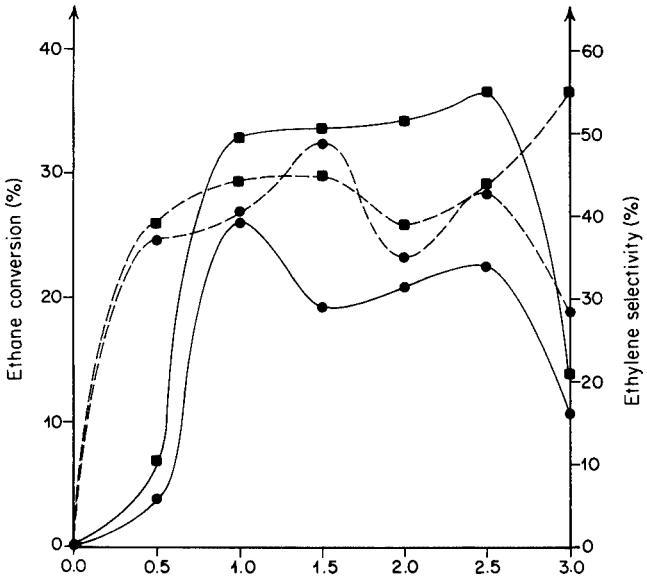

Figure 4. Ethane conversion (—) and ethylene selectivity (- - -) versus the $Co_xMg_{3-x}(PO_4)_2$ composition. The samples were calcined at 550 °C. The reaction temperature was (●) 500 and (■) 550 °C.

Table 2 reports ethane conversion and products selectivity at stationary state versus the phosphates composition at different temperatures of reaction and calcination. It shows that the activity increases with the reaction temperature. The optimal results are achieved when the samples are calcined at 550 °C. Figure 5 displays the ethylene selectivity versus the catalysts composition at 10% of conversion and different calcination temperatures. The curves display two maxima located at $x = 1.5$ and 2.5. The catalysts calcined at 700 °C showed lower performances than at 550 °C probably because the specific surface areas of the samples are lower.

The origin of these unusual maxima was attributed, as in the case of butan-2-ol conversion, to the composition and structural changes that the samples undergo when their cobalt content is modified. As a matter of fact, the bond length of the five-coordinated cobalt atoms Co(5)–Co(5) in $Mg_{1.5}Co_{1.5}(PO_4)_2$ and $Mg_{0.5}Co_{2.5}(PO_4)_2$ is equal to 2.980 Å, while in $MgCo_2(PO_4)_2$ and $Co_3(PO_4)_2$ it is equal to 3.00 and 3.062 Å, respectively [21]. The size of the ethane molecule is 2.44 Å [30]. Therefore, the solids that will best accommodate the bridged adsorption of C_2H_6 on two adjacent cobalt cations are those presenting the compositions $x = 1.5$ and 2.5 (figure 5). This adsorption of C_2H_6 is followed by the breaking of one of the C–H bonds to form adsorbed alkyl species which can lose another hydrogen and

Table 2
Performance of $Mg_{3-x}Co_x(PO_4)_2$ in ethane ODH.

x	Calcination temperature (°C)	Reaction temperature 500 °C			Reaction temperature 550 °C		
		α_g (%)	Selectivity (%)		α_g (%)	Selectivity (%)	
			C_2	CO_x		C_2	CO_x
0.5	550	4.0	37.0	63.0	7.1	38.9	64.1
0.5	700	8.6	6.2	93.8	11.0	9.3	90.7
1	550	26.3	29.9	70.1	33.0	44.6	55.4
1	700	8.0	10.3	89.7	9.3	12.2	87.8
1.5	550	19.3	48.9	51.1	33.6	44.8	55.2
1.5	700	11.6	39.2	60.8	19.6	47.4	52.6
2	550	21.0	35.5	64.5	34.6	39.2	60.8
2	700	8.3	30.5	69.5	10.6	24.6	75.4
2.5	550	22.7	43.1	56.9	36.6	44.4	55.6
2.5	700	13.1	40.3	59.7	18.3	58.1	41.9
3	550	10.7	28.9	71.1	13.6	55.3	44.7
3	700	6.6	18.6	81.4	9.3	32.4	67.6

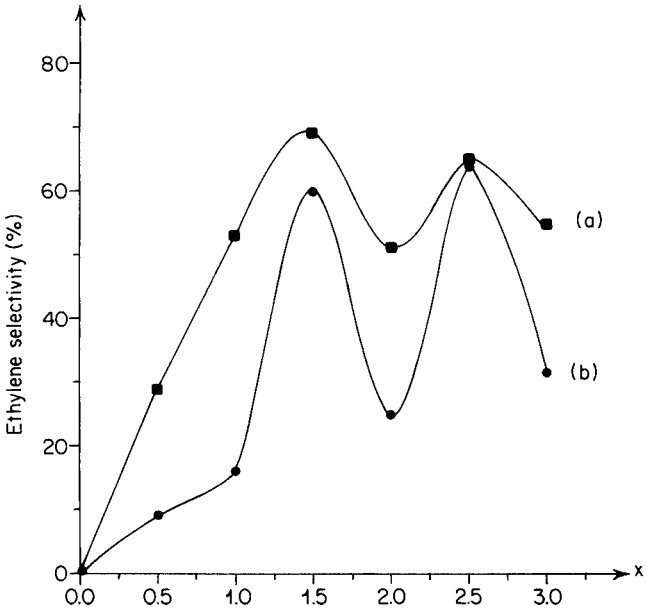

Figure 5. Ethylene selectivity at 10% of ethane conversion versus the catalysts composition. The reaction temperature was 550 °C and the samples were calcined at (a) 550 and (b) 700 °C.

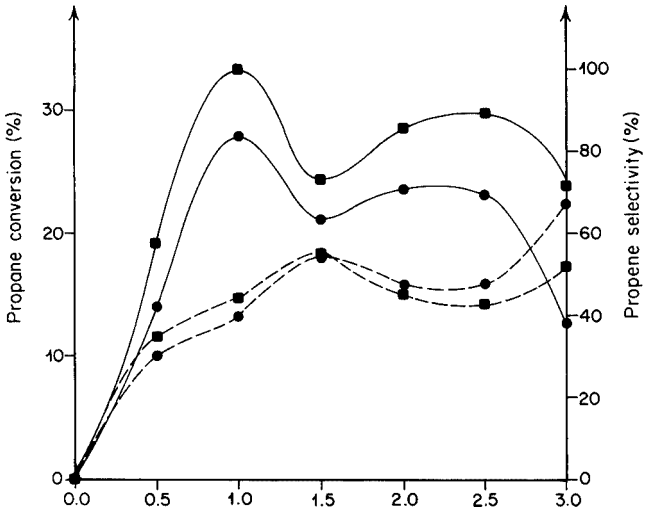

Figure 6. Propane conversion (—) and propylene selectivity (- - -) versus $Co_xMg_{3-x}(PO_4)_2$ composition. The samples were calcined at 550 °C and the reaction temperature was (•) 500 and (■) 550 °C.

then desorb as ethene. The phosphates that have Co(5)–Co(5) bond lengths exceeding 3 Å perform low ethylene selectivity. The cobalt cations located in the six-coordinated sites like in the most oxides, are essentially known to exhibit good combustion and hydrogenolysis properties [31].

The magnesium cations, as evidenced by the results, participate also in the mechanism of the reaction. They probably act as the centers that favor the formation of basic oxygen species which capture the hydrogen released by the ethane after the cleavage of the C–H bond [27]. This synergetic contribution of Mg^{2+} ions to the catalytic activity was confirmed by a complementary series of experiments which showed that the substitution of Mg^{2+} by Zn^{2+} in the same phosphates family leads to $Zn_{3-x}Co_x(PO_4)_2$ compounds which were found totally inactive in the oxidative dehydrogenation of the light alkanes in the investigated temperature range. This difference might in part be attributed to the fact that the proportion of cobalt in the five-coordinated sites Co(5) is much lower in $Zn_{3-x}Co_x(PO_4)_2$ than in $Mg_{3-x}Co_x(PO_4)_2$. The cobalt cations in the Co(5) sites represent around 73–74% in $Mg_{3-x}Co_x(PO_4)_2$ while this proportion in $Zn_{3-x}Co_x(PO_4)_2$ does not exceed 36–44% [32].

According to the literature, Co^{3+} ions might exist on the catalysts surface and hence be the source of the catalytic activity [33]. However, XPS, magnetic and UV-visible investigations of $Mg_{3-x}Co_x(PO_4)_2$ before and after the catalytic tests did not evidence such species or any noticeable modification of the phosphates structure.

3.4. Oxidative dehydrogenation of C_3H_8

Catalytic behavior of $Mg_{3-x}Co_x(PO_4)_2$ was also investigated in propane ODH. Figure 6 reports propane conversion and propylene selectivity versus the catalyst composition at 500 and 550 °C. The propane conversion displays two maxima located at $x = 1$ and 2.5. It also shows that the substitution of magnesium by cobalt in $Mg_3(PO_4)_2$ leads to active and selective phases. The best performances were achieved when the reaction was performed at 550 °C and the catalysts are calcined at 550 °C.

Table 3 summarizes the results collected at the stationary state. For $x = 1$ the conversion reaches 33% with selectivities toward propylene, ethylene and methane that are equal to 43.8, 6.3 and 1.2%, respectively.

For a better comparison of the catalysts performances, propylene selectivity versus the phosphates composition at 10% conversion and different calcination temperatures is represented in figure 7. The shape of this curve differs completely from that obtained for ethylene selectivity in ethane ODH (figure 5). It displays only a broad maximum around 77% for $x = 2$ when the sample is calcined at 550 °C. At a calcination temperature of 700 °C, this maximum disappears and after $x = 1$ the selectivity remains constant for all the compositions. Pure $Co_3(PO_4)_2$ has a selectivity around 60% at 10% of conversion.

The results, as in the case of ethane, seem to indicate that the reaction is sensitive to the catalysts composition. Therefore, as previously shown, the size of the hydrocarbon molecule has to be considered in order to understand the existence of the maxima observed in the activity and propylene selectivity. If it is assumed that prior to its dehydrogenation the hydrocarbon adsorbs via the hydrogen atoms C^{α}–H and C^{β}–H on two adjacent cobalt ions, the interatomic distance Co(5)–Co(5) has to be of approximately the same size as the propane molecule [30]. The ethane molecule is smaller than that of propane (3.27 Å) which is larger than any Co(5)–Co(5) bond length in $Mg_{3-x}Co_x(PO_4)_2$. The propane, as a result, will be less sensitive than ethane to the variations of the Co(5)–Co(5) interatomic distances, as shown in the figure 7. The cleavage of C^{α}–C^{β} bonds would obviously

Table 3
Activity and selectivity of $Mg_{3-x}Co_x(PO_4)_2$ in propane ODH.

x	Calcination temperature (°C)	Reaction temperature 500 °C					Reaction temperature 550 °C				
		α_g (%)	Selectivity (%)				α_g (%)	Selectivity (%)			
			C_3	C_2	C_1	CO_x		C_3	C_2	C_1	CO_x
0.5	550	13.9	30.2	0.7	0.1	69.0	19.4	34.5	1.5	0.4	63.6
0.5	700	10.6	50.1	1.2	0.1	48.6	11.6	45.3	2.0	0.1	52.6
1	550	28.1	39.9	2.8	0.4	56.9	33.3	43.8	6.3	1.2	48.7
1	700	5.7	52.6	0.7	–	46.7	8.5	50.6	2.4	–	47.0
1.5	550	21.2	55.7	5.2	0.5	38.6	24.3	55.6	6.6	1.6	36.2
1.5	700	18.3	43.2	2.2	0.2	54.4	24.7	38.9	3.2	0.4	57.5
2	550	23.8	47.5	2.5	0.3	49.7	28.6	46.2	3.8	0.6	49.4
2	700	11.7	50.4	1.7	0.1	47.8	14.4	54.2	2.8	0.3	42.7
2.5	550	23.4	47.9	3.4	0.4	48.3	29.9	42.8	4.4	1.0	51.8
2.5	700	15.0	44.0	2.0	0.3	53.7	24.0	34.6	2.1	0.4	62.9
3	550	13.0	67.7	3.1	0.2	29.0	24.1	51.9	3.3	0.4	44.4
3	700	15.0	28.7	1.3	0.1	69.9	17.7	37.3	1.7	0.2	60.8

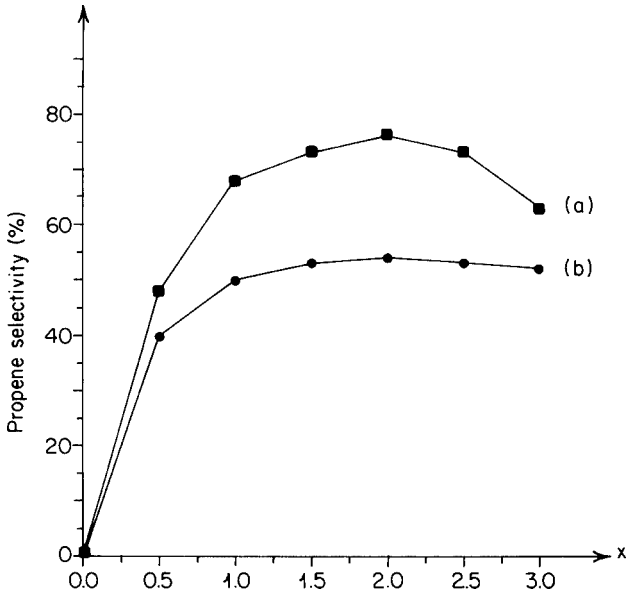

Figure 7. Propylene selectivity at 10% of propane conversion versus the catalysts composition. The reaction temperature was 550 °C and the samples were calcined at (a) 550 and (b) 700 °C.

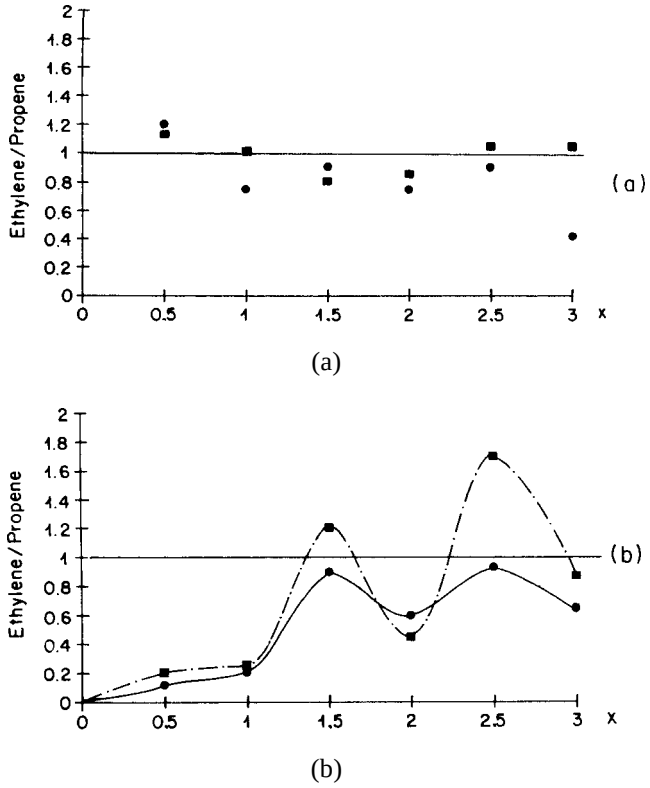

Figure 8. Ratios of ethylene and propylene selectivities ($S_{C_2=}/S_{C_3=}$) versus the catalysts composition at reaction temperatures (■) 500 and (●) 550 °C. The samples were calcined at (a) 550 and (b) 700 °C.

lead to the production of carbon oxides and methane. This analysis of the results is inspired by the multiplet theory formulated by Balandin and illustrated by Somorjai's studies [34,35]. It emphasises the importance of the "geometric factor" in the ODH of light hydrocarbons over the catalysts investigated.

To underline this influence of the catalysts structure on the activity and the selectivity, the ratio $S_{C_2=}/S_{C_3=}$ (ethylene selectivity/propylene selectivity) was plotted in figure 8 versus the phosphates composition. It shows that the major experimental data collected are located in the domain $S_{C_2=}/S_{C_3=} < 1$, confirming that the propane ODH is more selective than that of ethane in terms of alkenes production. The phenomena is more pronounced when the samples are calcined at 700 °C than at 550 °C. It might also be noted that ethylene selectivity becomes superior to that of propylene only for compositions which exhibit interatomic distance Co(5)–Co(5) shorter than 3 Å (i.e., for $x = 1.5$ and 2.5). Propane ODH produces propylene, ethane, methane and CO_x while ethane gives only ethylene and CO_x. In the case of propane, the thermodynamic stability of the reaction products and the hydrogenolysis properties of the cobalt are the main factors that lower the ODH performances in the specific conditions used.

4. Conclusion

The very stable phosphates of the solid solution $Mg_{3-x}Co_x(PO_4)_2$ ($0 \leqslant x \leqslant 3$) were prepared and found active and selective in the oxidative dehydrogenation of ethane and propane. Performances of this system in propane ODH were slightly superior to that of ethane. The results interpretation was based on the "geometric factor" and the interatomic Co(5)–Co(5) distances of the cobalt ions in the phosphate lattice.

Magnesium ions intervene in the mechanism of the reactions as promoters of the activity. They probably contribute in the regulation of the basic oxygen species that capture the hydrogen atoms released by the hydrocarbon.

Acknowledgement

The authors wish to express their grateful thanks to Professor J.C. Védrine and to the French Embassy in Rabat that partially funded this work under the Action Intégrée 99/183SM program.

References

[1] J.B. Moffat, Catal. Rev. Sci. Eng. 18 (1978) 199.
[2] A. Benarafa, M. Kacimi, G. Coudurier and M. Ziyad, Appl. Catal. A 196 (2000) 25.
[3] M. Kacimi, D. Amalric, F. Bozon-Verduraz and M. Ziyad, Phosphorus Res. Bull. 10 (1999) 442.
[4] M. Rouimi, M. Ziyad and J. Leglise, Phosphorus Res. Bull. 10 (1999) 418.
[5] P. Concepcion, J.M. Lopez Nieto and J. Perez-Pariente, Catal. Lett. 19 (1993) 333.
[6] J.B. Moffat and J.F. Neeleman, J. Catal. 31 (1973) 274.
[7] A. Clearfield, *Inorganic Ion Exchange Materials* (CRC Press, Boca Raton, FL, 1982).
[8] Y.Y. Huang, T.J. McCarthy and W.M.H. Sachtler, Appl. Catal. 148 (1996) 135.
[9] L. Jinlin and N.J. Coville, Appl. Catal. 181 (1999) 201.
[10] H. Kraus and R. Prins, J. Catal. 170 (1997) 20.
[11] M.A. Keane and G. Webb, J. Mol. Catal. 73 (1992) 91.
[12] Y. Takita, K. Sano, K. Kurosaki, N. Kawata, H. Nishigushi, M. Ito and T. Ishihara, Appl. Catal. 167 (1998) 49.
[13] J. El-Idrissi, M. Kacimi, F. Bozon-Verduraz and M. Ziyad, Catal. Lett. 56 (1998) 221.
[14] J. El-Idrissi, M. Kacimi, M. Loukah and M. Ziyad, J. Chim. Phys. 94 (1997) 1984.
[15] B.K. Hodnett, Catal. Today 1 (1981) 477.
[16] C. Kemball, Adv. Catal. 11 (1959) 225.
[17] N. Cheikhi, M. Ziyad, G. Coudurier and J.C. Védrine, Appl. Catal. A 118 (1994) 187.
[18] T. Koerts, M.J.A.G. Deelen and R.A. van Santen, J. Catal. 138 (1992) 101.
[19] M. Loukah, G. Coudurier, J.C.Védrine and M. Ziyad, Micropor. Mater. 4 (1995) 345.
[20] A.G. Nord, Mater. Res. Bull. 12 (1977) 563.
[21] A.G. Nord and T. Stefanidis, Z. Kristallogr. 153 (1980) 141.
[22] M. Cimpolini and M. Nardi, Inorg. Chem. 5 (1966) 41.
[23] P. Gajardo, P. Grange and B. Delmon, J. Phys. Chem. 83 (1979) 1771.
[24] J. Le Bars, A. Auroux, M. Forissier and J.C. Védrine, J. Catal. 162 (1996) 250.
[25] M. Kacimi and M. Ziyad, J. Chim. Phys. 94 (1997) 2007.
[26] T. Yamanaka and K. Tanabe, J. Phys. Chem. 80 (1976) 1723.
[27] E. Giamello, E. Garrone, S. Coluccia, G. Spoto and A. Zecchina, in: *New Developments in Selective Oxidation*, eds. G. Centi and F. Trifirò (Elsevier, Amsterdam, 1990).
[28] A.G. Nord, Mater. Res. Bull. 17 (1982) 1001.
[29] H.H. Kung, Adv. Catal. 40 (1994) 1.
[30] P.M. Michalakos, M.C. Kung, I. Jahan and H.H. Kung, J. Catal. 140 (1993) 226.
[31] E. Finocchio, R.J. Willey, G. Ramis, G. Busca and V. Lorenzelli, Stud. Surf. Sci. 101 (1996).
[32] A.G. Nord, Acta Crystallogr. B 40 (1984) 191.
[33] G. Tulyev and S. Angelov, Appl. Surf. Sci. 32 (1988) 381.
[34] A.A. Balandin, Adv. Catal. 19 (1969) 1.
[35] G.A. Somorjai, *Principle of Surface Chemistry and Catalysis* (Wiley, New York, 1994).